INFECTION AND IMMUNITY, Dec. 1996, p. 5053–5060 Vol. 64, No. 12
0019-9567/96/$04.00+0

Magnetic Resonance Imaging and Histopathological Study of Brain Lesions in Rabbits Given Intravenous Verotoxin 2

JUN FUJII,[1]* YOSHIMASA KINOSHITA,[2] TOSHIRO KITA,[3] AIICHIRO HIGURE,[4] TAE TAKEDA,[5] NORIYUKI TANAKA,[3] AND SHIN-ICHI YOSHIDA[1]

Department of Microbiology,[1] Department of Neurosurgery,[2] Department of Forensic Medicine,[3] and Department of General and Abdominal Surgery,[4] School of Medicine, University of Occupational and Environmental Health, Kitakyushu 807, and Department of Infectious Disease Research, National Children's Medical Research Center, Tokyo 154,[5] Japan

Received 28 May 1996/Returned for modification 7 August 1996/Accepted 18 September 1996

When rabbits were given intravenously purified verotoxin 2 (VT2) at 5 μg/kg of body weight, they developed hemorrhagic diarrhea, flaccid paresis, an ataxic gait, an opisthotonic posture, and convulsions. To examine the effects of VT2 toxemia on the rabbit central nervous system, magnetic resonance imaging and ultrastructural studies were performed. At 24, 57, and 80 h after injection of VT2 into 12 rabbits, T2-weighted images of the central nervous system were obtained. The initial lesion was noted at 24 h in the hypothalamic areas of all experimental animals. At 57 h, the T2 value increased in the medulla of the cerebral hemisphere or the hippocampus, with a brain stem lesion in six rabbits (50%). The rabbits with the brain stem lesions, in which neurological signs were very severe, died within 6 days. Lesions in the cerebellar hemisphere and/or vermis were noted in four rabbits (33%) that survived more than 1 month. To better understand the pathogenesis of VT2 in these brain lesions, we examined the deterioration of the blood-brain barrier and cerebrospinal fluid-brain barrier by using horseradish peroxidase as a tracer. The tracer was detected by electron microscopy both in the subendothelial layer, including the basal lamina, and throughout the cytoplasm of the ependymal cell layer covering the ventricle after intravenous or intrathecal treatment with horseradish peroxidase. We also determined the localization of VT2 by immunoelectron microscopy and found that it was localized on edematous endothelial cells of capillaries, ependymal cells, and myelin sheaths. The present study suggests that VT2 was conveyed from the endothelial and ependymal cell layers and caused edematous changes in the rabbit brain.

Verotoxin (VT)-producing *Escherichia coli* (VTEC) infection has been reported to be associated with hemorrhagic colitis (27), hemolytic uremic syndrome (HUS) (13, 14), and thrombotic thrombocytopenic purpura (22) in humans. VTEC strains produce VT1, VT2, and variants of VT2, i.e., VT2e and VT2c. Strains producing VT1, VT2, and VT2c have been associated with HUS and thrombotic thrombocytopenic purpura in humans (reviewed in references 12 and 22), whereas VT2e-producing strains cause edema disease in pigs (17). VT1 and VT2 inhibit the protein synthesis of eukaryotic cells in the same way as Shiga toxin does (reviewed in reference 12). VT1 is virtually identical to Shiga toxin (31, 32), while VT2 shows 56% homology to VT1 at the amino acid sequence level (11). Nucleotides of VT2 and VT2c are 98% homologous in the B subunits (9), whereas VT2e has 91% DNA sequence homology with VT2 (39). VT1 and VT2 have been known to bind the glycolipids globotriosylceramide (Gb_3) as functional receptors (18, 38). Shiga toxin and VTs have been shown to be directly toxic for human vascular endothelial cells in vitro (33).

Shigella dysenteriae type 1 has caused ekiri, an acute encephalopathy associated with bacillary dysentery, in Japanese children (16). The neurotoxicity of Shiga toxin, however, has been considered to be a secondary effect caused by the damage to the vascular endothelial cells in the central nervous system (CNS) (4, 10). The CNS of humans is affected by VTEC infection (7, 12), and CNS complications are an important predictive factor for HUS mortality in children (28, 37). In an outbreak of VTEC infection in Urawa City, Japan, in 1990, two children who showed neurological symptoms, including convulsion and coma, died before the development of HUS (7).

Animal models have been developed to analyze CNS damage due to VTEC infection. The brain stem, cerebrum, and cerebellum of piglets challenged with *E. coli* producing VT1 and/or VT2 contained areas of necrosis and malacia (5). In 1989, Barrett et al. (3) reported that rabbits developed motor incoordination and paresis when VT2 was given intravenously, and brain lesions were observed in the CNS of the rabbits by light microscopy. Following these results, Richardson et al. (25) reported in 1992 that when rabbits were challenged intravenously with VT1, the accumulation of VT1 in the CNS was significantly higher than that in other organs, and they suggested that the brain lesions were caused by vasculopathy rather than by a direct toxicity of VT1 against nerves. After establishing a mouse model of CNS disorder by oral infection with VT2c-producing *E. coli*, we (6) found that VT2c was toxic to both the endothelial cells of capillaries and nerve fibers in the brain cortex and spinal cord in the mice. Using a tracer, we showed the destruction of the blood-brain barrier (BBB) by detecting the tracer extravasation. Although neural damage induced by VTs has been considered to be a result of microvascular damage, we suggested that VT2c had a direct cytotoxic effect on neurons (6).

Magnetic resonance imaging (MRI) is definitely more sensitive than X-ray computed tomography in detecting brain edema, demyelination, and primary traumatic brain damage.

* Corresponding author. Mailing address: Department of Microbiology, School of Medicine, University of Occupational and Environmental Health, Kitakyushu 807, Japan. Phone: 81-93-691-7242. Fax: 81-93-602-4799. Electronic mail address: jfujii@med.uoeh-u.ac.jp.

TABLE 1. Experimental design

Expt no.	Method	No. of animals injected with:	
		VT2	Saline (controls)
1	MRI clinical study	12	0
2	Light and transmission electron microscopy	12	3
3	Tracer expt	4[a]	4[a]
4	Immunohistochemical study	2	2

[a] Two of the four rabbits were injected with HRP intravenously, and the other two were injected intrathecally.

Unlike with computed tomography, signals from bones do not interfere with MRI. T2-weighted images on MRI provide much information on vasogenic edema and demyelination (e.g., in multiple sclerosis [20]). Furthermore, T2-weighted images are sensitive in detecting lacunar infarction that consists of degenerated nerve fibers and gliosis. By using the MRI technique in the present study, we attempted to detect brain lesions in rabbits induced by VT2.

In humans, VT2-producing *E. coli* strains tend to be isolated from patients with the development of HUS and thrombotic thrombocytopenic purpura (21, 24). Tyler et al. (35) reported that a significant number of O157:H7 isolates possess the VT2v genotype. Tzipori et al. (36) detected lesions histologically in the cerebral cortex, thalamus, and cerebellum in a human baby who died after infection with VT2-producing *E. coli*. We paid special attention to the clinical course of VTEC infection in children who had developed severe neurological manifestations (coma, convulsion, etc.) culminating in death (7). They did not have any gross lesions as determined by computed tomography or autopsy.

In this study, we used a rabbit model with VT2 given intravenously. Comparing the MRI images with results of tracer experiments and immunoelectron microscopic features, we investigated the sites and time courses of brain damage and pathological changes of the CNS.

MATERIALS AND METHODS

Purified VT2. VT2 was purified from a culture supernatant of *E. coli* C600 (933W) by the method described by Yutsudo et al. (40). The biological activity of the VT2 was monitored by cytotoxicity on Vero cells to determine the 50% cytotoxic dose. The activity was approximately 10^6 50% cytotoxic doses per μg of protein, in which one 50% cytotoxic dose is defined as the amount of VT2 activity required to produce a 50% cytopathic effect in a Vero cell monolayer after 3 days of incubation at 37°C.

Animals. The Japanese White rabbits, weighing 2 kg each, used in this study were purchased from Shizuoka Experimental Animals, Hamamatsu, Japan. A total of 39 male rabbits were used in this study.

Experimental design. We divided the experiments into four groups according to the experimental methods. The numbers of rabbits for each experiment are shown in Table 1.

(i) Experiment 1 (MRI clinical study). To observe the clinical effects of VT2, 12 rabbits were challenged intravenously with 5 μg of VT2 per kg of body weight in a 2-ml solution via a marginal ear vein. The rabbits were housed in individual cages with a 12-h light-dark cycle and were permitted food and water ad libitum. Testing of occult blood in the stool was done with Hematest II (Bayer-Sankyo Co. Ltd., Tokyo, Japan). Since it is important to immobilize the animals for in vivo MRI studies, the animals were anesthetized by an intravenous injection of pentobarbital (Nembutal, 50 mg/ml; Dabbot Co.) at approximately 0.5 ml/kg. Although MRI provided abnormal images at 24, 57, and 80 h after VT2 injection, the animals were not sacrificed and investigated for the effect of VT2 on mortality. Three animals given sterile saline intravenously were used as controls. We observed brain edema for 1 month by the MRI technique. MRI was performed with a 4.7-T-MR system (SIS 200/400; Spectroscopy Imaging Systems Corp., Fremont, Calif.) with a 400-mm horizontal bore and a proton frequency of 200.0 MHz. Spin-echo MR images were obtained in orthogonal planes to confirm the desired positionings. The acquisition parameters for coronal T2-weighted images were as follows: repetition time, 2,500 ms; echo time, 80 ms; field of view, 80 by 80 mm; matrix, 256 by 192; two excitations averaged; and 11 2-mm coronal slices with a 0.5-mm gap. Those for sagittal T2-weighted images were the same except that the 11 2-mm coronal slices were without center-to-center spacing.

(ii) Experiment 2 (light and electron microscopic studies). For microscopic studies, 12 other rabbits were challenged intravenously with 5 μg of VT2 per kg via the marginal ear vein, and then the brain tissues where abnormalities were observed in MRI were examined by light and electron microscopy.

(a) Perfusion fixation. The rabbits were perfused transcardially (110 mm Hg) with a solution of sterile saline (37°C) and then with a mixture of 4% paraformaldehyde and 0.5% glutaraldehyde in 0.1 M phosphate-buffered saline (PBS) at 4°C by using a perfusion fixational device (Nissin EM Co. Ltd., Tokyo, Japan) (19). This perfusion fixation was performed for light and electron microscopic studies, tracer experiments, and immunocytochemistry. For light and transmission electron microscopy, 12 animals given VT2 and three controls given sterile saline intravenously were perfused and fixed as described above.

(b) Light microscopic study. After brains were removed and dissected, all specimens were embedded in paraffin. Approximately 6-μm-thick sections were cut and stained by the hematoxylin-and-eosin method, Bodian's silver impregnation, and the Klüver-Barrera method.

(c) Electron microscopic study. The brain tissues where abnormalities had been observed in MRI were isolated and divided into five parts: the medulla of the cerebral hemisphere, the hippocampus, the vermis of the cerebellum, the brain stem, and the hypothalamus. All parts were cut into 2-mm-thick slices and immersed in a mixture of 4% paraformaldehyde and 0.5% glutaraldehyde in 0.1 M PBS for 1 h at 4°C. Approximately 30- to 40-μm-thick sections were made on a microslicer (Dosaka EM Co. Ltd., Osaka, Japan) and inserted into a sample mesh pack (Shiraimatsu & Co. Ltd., Osaka, Japan). Specimens were postfixed in 2% osmium tetroxide in 0.1 M PBS for 1 h at 4°C, and then all specimens were dehydrated in an ascending ethyl alcohol series and embedded in Quetol 812. Ultrathin sections were stained with uranyl acetate and lead citrate and examined in a JEM 1200 EX electron microscope.

(iii) Experiment 3 (tracer experiment). For each tracer experiment, four rabbits were used.

(a) Intravenous injection of HRP. Two rabbits at 24 h after the injection of VT2 and two controls at 24 h after the injection of sterile saline were pretreated intraperitoneally with 50 mg of diphenhydramine hydrochloride per kg to prevent histamine release and were injected intravenously with 45 mg of horseradish peroxidase (HRP) (type VI; Sigma Chemical Company, St. Louis, Mo.) via a marginal ear vein according to the method of Karnovsky (15). At 10 min after the HRP injection, the animals were perfused and fixed as described above. The hypothalamus around the third ventricle was cut into approximately 2-mm-thick slices and postfixed in the same fixative for 1 h. Sections approximately 30 to 40 μm thick were made on a microslicer (Dosaka EM Co.) and inserted into a sample mesh pack (Shiraimatsu & Co.). They were treated with a solution of 3,3′-diaminobenzidine tetrahydrochloride in 0.05 M Tris buffer containing 0.05% H_2O_2 for 10 min at room temperature, thoroughly washed in 0.05 M Tris buffer, postfixed in 1% osmium tetroxide in 0.1 M PBS for 1 h at 4°C, dehydrated in an ascending ethyl alcohol series, embedded in Quetol 812, and examined in an electron microscope.

(b) Intrathecal injection of HRP. Two rabbits at 24 h after the injection of VT2 and two controls were injected into the cerebrospinal fluid space from the cisterna magma with 9 mg of HRP in 0.4 ml of saline at 37°C very slowly (over a 5-min period) through a 27-gauge needle (diameter, 0.40 mm; length, 19 mm) attached to a syringe. At 10 min after the HRP injection was finished, the animals were fixed by vascular perfusion as described above, and then the hypothalamus around the third ventricle was cut and postfixed for the tracer examination as described above and examined in an electron microscope.

(iv) Experiment 4 (immunohistochemical study). For immunocytochemistry, four rabbits were used.

(a) Antibodies. For immunocytochemistry, we used a monoclonal antibody made by immunizing mice with VT2 detoxified by treatment with 1% formalin in 0.1 M phosphate buffer (pH 8.0) at 37°C for 3 days. The monoclonal antibody Vm 1.1 specific for VT2 (purified immunoglobulin G, 0.95 mg/ml) was prepared and kindly provided by Teijin Ltd. (Hino, Tokyo, Japan). We then verified by enzyme-linked immunosorbent assay that the monoclonal antibody reacted with VT2 (50 ng/50 μl) at a dilution higher than 1:16,000.

(b) Immunostaining procedures. The streptavidin-biotin technique of Shi et al. (29) was used. Two rabbits at 57 h after the injection of VT2 and two controls were perfused as described above. The brain sections were cut into approximately 2-mm-thick slices and postfixed in the same fixative for 1 h. Sections approximately 30 to 40 μm thick were made on the microslicer and inserted into the sample mesh pack. The endogenous peroxidase activities were blocked by incubation in a periodic acid solution (Histofine, no. 29271; Nichirei Co. Ltd., Tokyo, Japan) for 45 s. After treatment with normal goat serum at room temperature, sections were incubated overnight with the above-mentioned primary antibody at 4°C. The sections were incubated with a biotinylated secondary antibody [goat anti-mouse immunoglobulin $F(ab')_2$; EY Laboratories, Inc.], which was diluted to 1:200 with 0.05 M Tris buffer, for 1 h at 37°C and then with a streptavidin-peroxidase complex (Histofine SAB-PO kits; Nichirei Co. Ltd.), diluted to 1:600 with 0.05 M Tris buffer, for 1 h at 37°C. After incubation, the sections were treated with 3,3′-diaminobenzidine tetrahydrochloride in 0.05 M

TABLE 2. Clinical features and MRI findings in rabbits given VT2

Severity of clinical features	No. of animals	CNS lesions detected by T2-weighted imaging
Mild[a]	2	Around third ventricle (involving hypothalamus)
Moderate[a,b]	4	Around third ventricle (involving hypothalamus); cerebellar vermis and/or hemisphere
Severe[a,c]	6[d]	Around third ventricle (involving hypothalamus); brain stem; cerebrum or hippocampus[e]

[a] Weakness, weight loss, and hemorrhagic diarrhea.
[b] Ataxic gait and opisthotonic posture.
[c] Paralysis of extremities and convulsion.
[d] All six rabbits died.
[e] Four rabbits showed cerebral lesions, and two rabbits showed hippocampal lesions.

Tris buffer containing 0.05% H_2O_2 (pH 7.6) for 10 min at room temperature. They were thoroughly washed in 0.05 M Tris buffer, postfixed in 1% osmium tetroxide for 1 h at 4°C, dehydrated in an ascending ethyl alcohol series, embedded in Quetol 812, and examined in the electron microscope.

For controls for each immunostaining, Tris buffer or medium used for culturing hybridoma cells was substituted for the primary antibodies.

RESULTS

Experiment 1. (i) Clinical features. All of the 12 rabbits given VT2 suffered from weakness, weight loss, and hemorrhagic diarrhea. Six rabbits (50%) developed paralysis of the extremities and convulsions, culminating in death within 4 days. Four rabbits (33%) developed an ataxic gait and an assumed an opisthotonic posture, but they remained alive for 1 month. Two rabbits (16.7%) showed no neurological signs and remained alive for more than 1 month (Table 2). The other 12 rabbits, given VT2 and sacrificed for microscopic studies, also showed clinical signs similar to those of the first 12 rabbits described above.

(ii) MRI findings. Figure 1A shows a T2-weighted image at the midsagittal level, and Fig. 1B shows a coronal T2-weighted image at the third ventricle level, for the nontreated control rabbits. Figure 1C shows a coronal MRI for the treated rabbits at the third ventricle level at 24 h after injection of VT2. The area surrounding the third ventricle (arrowhead) increased in signal intensity in all animals compared with controls. The lesions, including that in the hypothalamus, developed more extensively over time. At 57 h after injection of VT2, the four animals also showed an area of signal hyperintensity (arrow) in the brain stem (Fig. 1D). At 57 h after VT2 injection, the medulla of the cerebral hemisphere appeared to be hyperintense (Fig. 1E) in four animals. The bilateral or unilateral hippocampus appeared to be hyperintense after 57 h in 2 of the 12 animals (data not shown), with an area of hyperintensity in the brain stem. At 80 h after the injection of VT2, the vermis appeared to be hyperintense (Fig. 1F, arrowhead) in 4 of the 12 treated animals. These four animals developed an ataxic gait, paralysis of the extremities, and an opisthotonic posture. The high signal intensity in the cerebellar hemisphere was recognized at 1 month after VT2 injection. Table 2 shows the association of clinical features and the distribution of abnormal lesions detected by MRI.

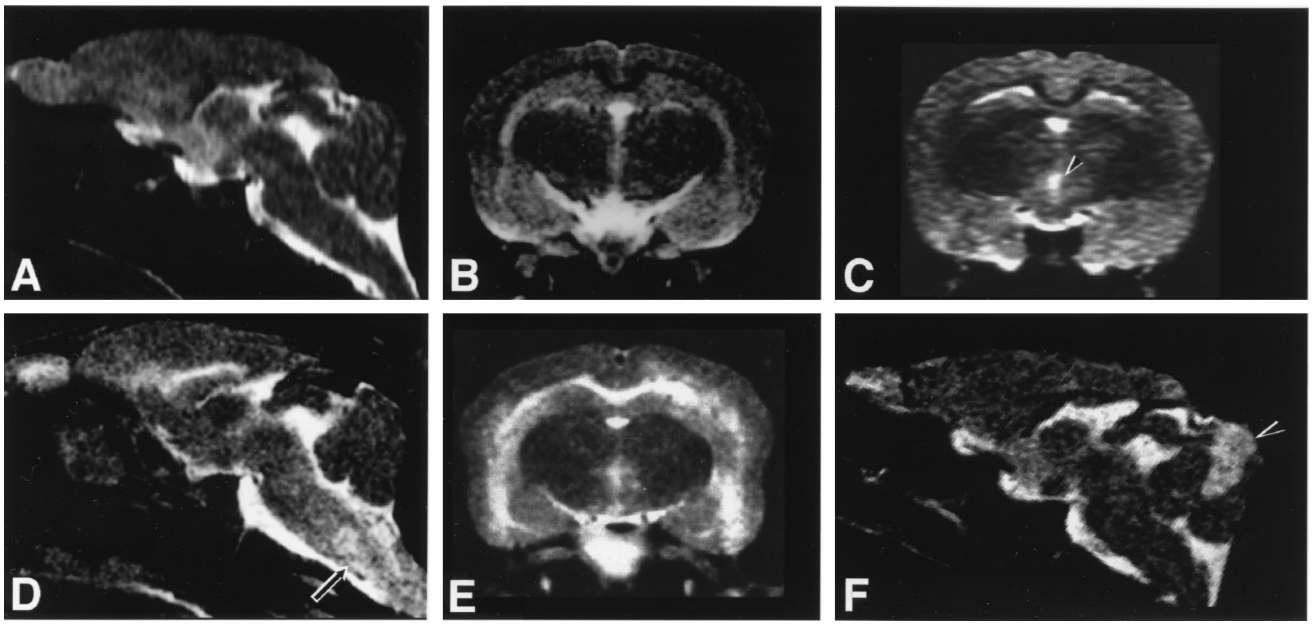

FIG. 1. MRI of the brains of normal and VT2-challenged rabbits. (A) Midsagittal T2-weighted image of a control rabbit's brain. (B) Coronal T2-weighted image at the third ventricle level of a control rabbit's brain. (C) T2-weighted image at 24 h after VT2 administration. A high signal intensity around the third ventricle is seen (arrowhead) in a coronal T2-weighted image at the third ventricle level. (D) T2-weighted image at 57 h after VT2 administration. A midsagittal T2-weighted image reveals a high signal intensity in the brain stem (arrow). (E) T2-weighted image at 57 h after VT2 administration. A coronal T2-weighted image shows a high signal intensity in the medulla of the cerebral hemisphere at the third ventricle level. (F) T2-weighted image at 80 h after VT2 administration. A midsagittal T2-weighted image of the cerebellum shows a high signal intensity (arrowhead).

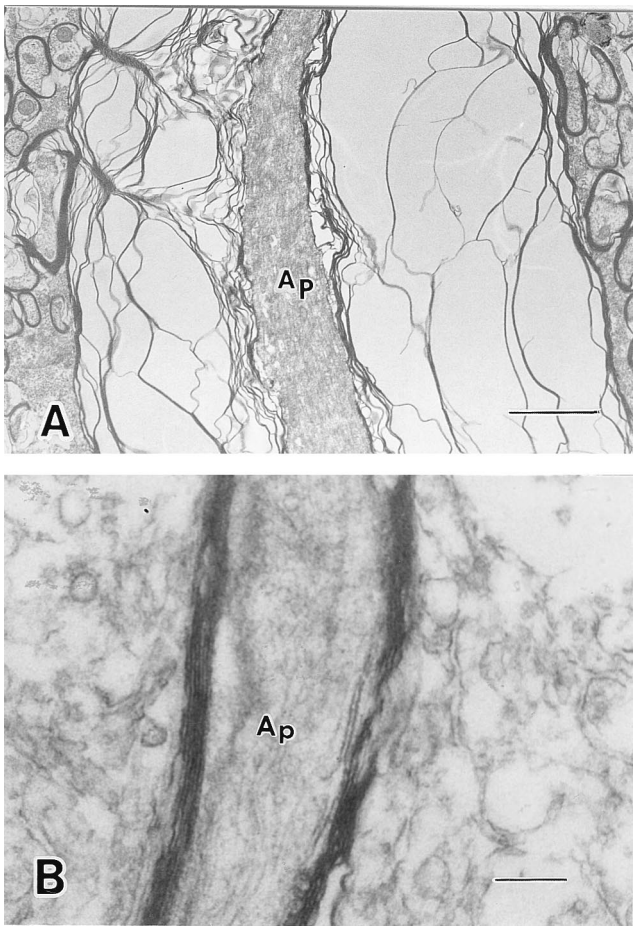

FIG. 2. (A) Electron micrograph showing a vacuolated myelin sheath in the brain stem lesion area of a treated animal at 57 h after VT2 administration. The axoplasm (Ap) of the vacuolated fiber appears to be normal. Bar, 2 μm. (B) Electron micrograph showing a normal myelin sheath in the brain stem of a control animal. Bar, 200 nm.

FIG. 3. Electron micrograph from a tracer experiment showing a capillary in the hypothalamic lesion area of a treated animal at 24 h after VT2 administration. The tracer HRP is localized in the subendothelial space (arrow) including the basement membrane (arrowhead). Bar, 500 nm.

Experiment 2. (i) Light microscopic findings. In the lesions of the brain stem and the medulla of the cerebral hemisphere, swelling and waving of axons were evident, and degenerative changes in the myelin sheath were found along the axoplasm (data not shown). Myelinic degeneration and myelin globoids were also found, but obvious axonal retraction balls were not detected. In the neural cell bodies, Nissl bodies disappeared and tigrolysis was observed. Neural cells looked globular and spindle shaped, and a strong degenerative change was observed. The number of glial cells also increased remarkably in all of the brain lesions that were examined.

(ii) Electron microscopic findings. At 24 h after the injection of VT2, edematous changes in the ependymal cells covering the third ventricle became pronounced. The cells also contained an abundance of intracytoplasmic vacuoles in the apical cytoplasm. During this period, endothelial cells of the capillaries and astrocytes forming the vascular feet around the endothelium in the hypothalamus also became slightly edematous, and the numbers of vacuoles and pinocytotic vesicles were increased compared with those in the controls. At 57 h after injection, edematous changes became pronounced in the endothelial cells and the surrounding astrocytes forming the vascular feet in the areas around the third ventricle, the medulla of the cerebral hemisphere, and the brain stem. There was a progressive degeneration of myelinated nerve fibers and neural cell bodies in these areas. At 80 h after injection, the degeneration of neural cell bodies and myelinated nerve fibers was also observed in the cerebellar vermis. In the brain stem lesion, a wide destroyed space in the myelin sheath (Fig. 2A) was discovered compared with controls (Fig. 2B).

Experiment 3 (tracer experiment). To investigate the permeability of the BBB, we injected HRP via an ear vein in the rabbits that had been given VT2 intravenously. At 24 h after VT2 administration, the tracer was localized in the subendothelial space including the basement membranes of capillaries in the hypothalamic lesion areas (Fig. 3). This suggests that VT2 increased the permeability of capillaries and impaired the BBB. The tracer could not be detected in the subendothelial spaces and basement membranes of capillaries in the brains of control rabbits injected with saline. Furthermore, we injected HRP into the cerebrospinal fluid space, i.e., into the cisterna magma, and investigated the ependymal cells around the third ventricle. At 24 h after VT2 administration, the HRP was distributed throughout the cytoplasm of the ependymal cells (Fig. 4A). This suggests that VT2 impaired the cerebrospinal fluid-brain barrier (CBB). In the controls, the tracer was localized only in the lysosomes of ependymal cells (Fig. 4B).

Experiment 4 (immunohistochemical study). To determine the localization of VT2, we performed an immunochemical study. Immunoreactions existed on the apical plasma membranes of endothelial cells of the hypothalamic capillaries (Fig. 5A) and lysosomes of ependymal cells in hypothalamic lesion areas (data not shown) at 24 h after injection of VT2. We could detect immunoreactions of VT2 in the myelin sheaths of myelinated nerve fibers in the lesion areas of the medulla of the cerebral hemisphere and the brain stem (Fig. 5B) at 57 h after injection of VT2.

DISCUSSION

Our study indicated that the primary lesion of the brain occurred in the hypothalamic area when rabbits were given VT2. At 24 h after the injection of VT2, MRI showed a high intense signal in this area on T2-weighted images (Fig. 1C). The electron microscopy demonstrated significant cell damage to the ependymal cells of the third ventricle, which showed

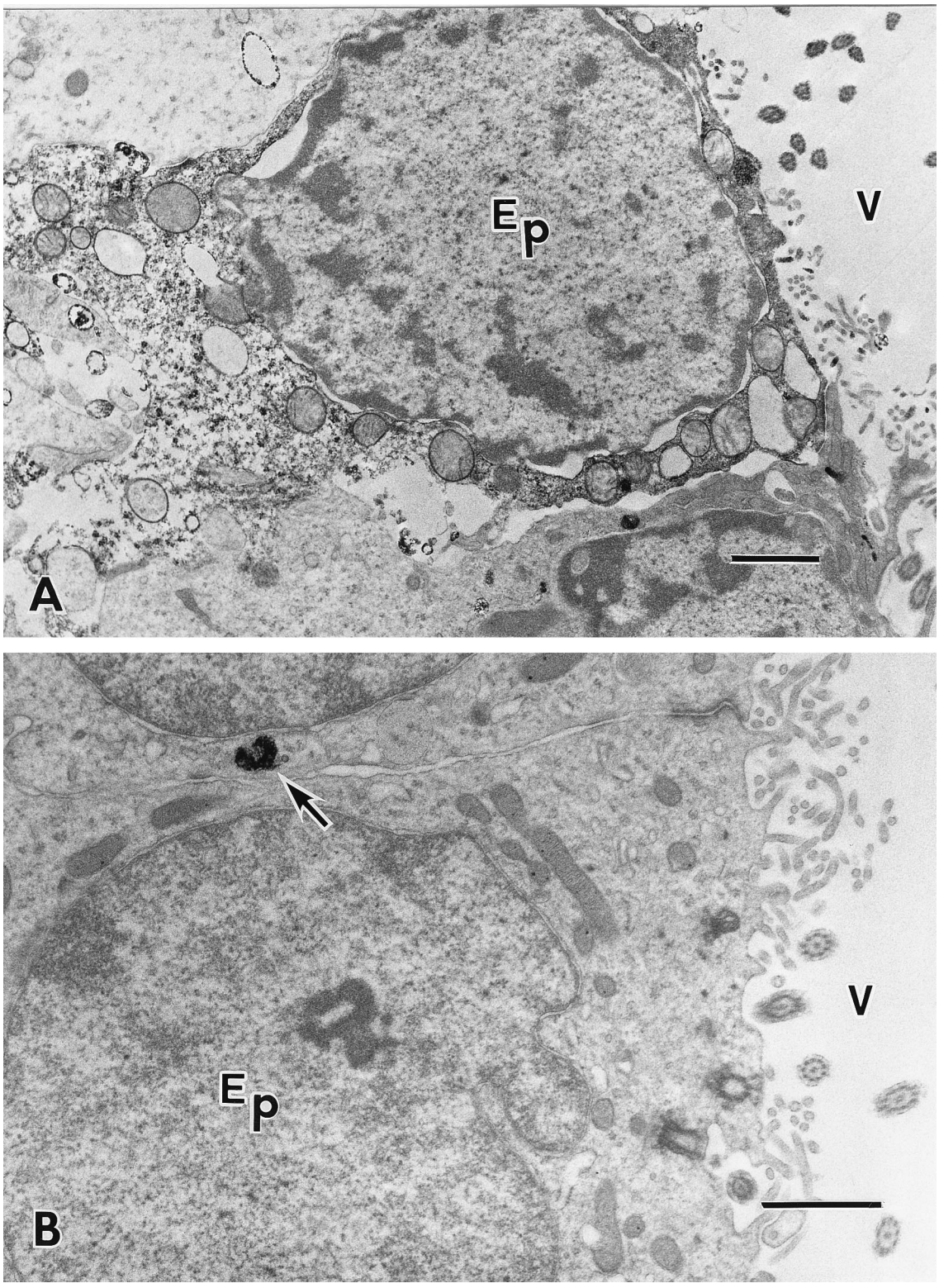

FIG. 4. Electron micrographs from a tracer experiment showing the ependymal cells (Ep) around the third ventricle (V). (A) The HRP is distributed throughout the cytoplasm of an ependymal cell of a treated animal at 24 h after injection of VT2. Bar, 500 nm. (B) Normal ependymal cells around the third ventricle of a control animal. The HRP is localized in the lysosomes of an ependymal cell (arrow). Bar, 1 μm.

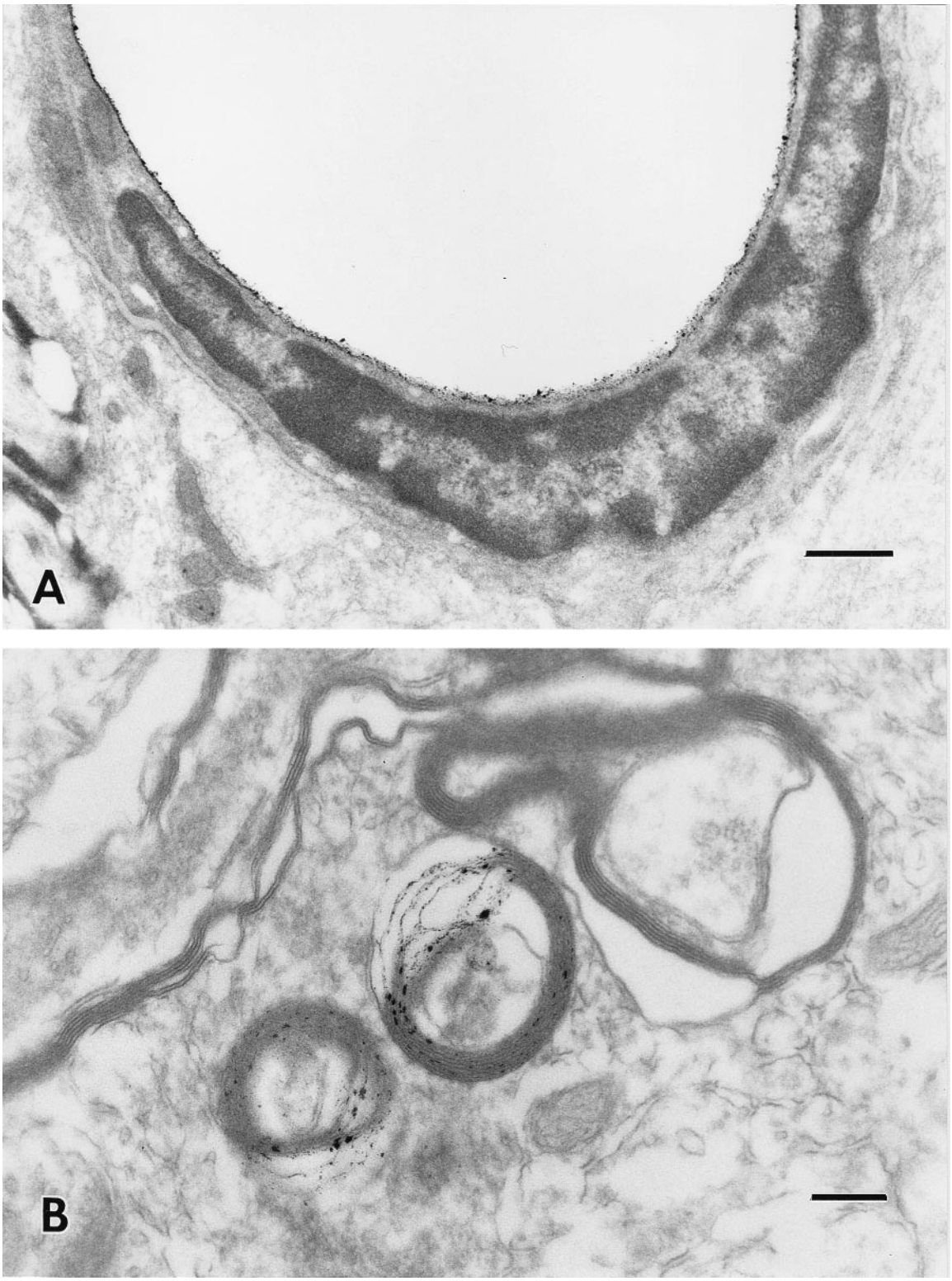

FIG. 5. (A) Electron micrograph showing immunoreactions of VT2 on the apical plasma membrane of an endothelial cell of the capillary in the hypothalamic lesion area of a treated animal at 24 h after injection of VT2. Bar, 500 nm. (B) Electron micrograph showing immunoreactions of VT2 in the myelin sheaths of myelinated nerve fibers in the brain stem lesion area of a treated animal at 57 h after injection of VT2. Bar, 200 nm.

edematous changes, including an abundance of intracytoplasmic vacuoles in the apical cytoplasm (Fig. 4A). The ependymal cell layer has a tight junction that mainly acts as the CBB, although the tight junction of the CBB is not as strong as the BBB. The tracer experiments suggest that the influx of VT2 into the cerebrospinal fluid causes injury of the tight junction between ependymal cells and results in destruction of the CBB (Fig. 4A). In the case of capillaries, the tracer was localized in the subendothelial space including the basement membrane (Fig. 3). This suggests that VT2 impaired the BBB the same as the CBB. The immunoreactions of VT2 in the lysosomes of ependymal cells imply the invasion of VT2 from the cerebrospinal fluid. On the basis of our results up to now, we suggest that intravenous VT2 invades the rabbit CNS through the BBB and CBB and begins to cause brain damage where MRI shows abnormal signal intensities, in the hypothalamic area around the third ventricle.

Following the damage to the ependymal cell layer, the increased signal intensity was observed in the brain stem on T2-weighted images along with lesions of the medulla of the cerebral hemisphere (Fig. 1E) and hippocampus. In this study, one of the most notable findings is that the extension of the brain stem lesion revealed by the MRI (Fig. 1D) is correlated with the mortality rate (Table 1). By electron microscopy, we observed the destruction of the arrangement of the myelin sheaths in the brain stem (Fig. 2A), the medulla of the cerebral hemisphere, and the cerebellum. Furthermore, we could detect immunoreactions of VT2 in the destroyed myelin sheaths in the medulla of the cerebral hemisphere and the brain stem (Fig. 5B). These findings imply that VT2 induced strong and direct cytotoxic effects on myelinated nerve fibers. We suggest that the nerve fiber destruction in the brain stem induced by VT2 plays a crucial role in the death of rabbits.

Barrett et al. (3) reported that in rabbits given VT2, changes in the cerebrum and brain stem seen by light microscopy were minimal and spinal cord lesions were dominant and that these lesions were due to hemorrhage and necrosis of neural cells. In earlier works, we also reconfirmed the hemorrhage and necrosis of neural and endothelial cells of the brain in rabbits given VT2 intravenously when the tissues were fixed in 10% buffered neutral formalin without perfusion fixation (unpublished data). Barrett et al. (3), however, did not perform an electron microscopic examination, including immunocytochemistry and tracer experiments. In a previous histopathological study of rabbits after intravenous administration of VT1, Richardson et al. (25) showed that edema and hemorrhaging in the brain and the spinal cord were evident, and VT1 was detected in the blood vessels of the spinal cord by the immunofluorescence technique. They used specific fibrin stains and found that the fibrin thombi affected the vascular wall and that the brain lesions showed edema, hemorrhage, and infarction in the entire gray matter. Zoja et al. (41) reported that pericellular and perivascular edema, focal hemorrhaging, and vascular lesions were fundamental findings in rabbits given VT1. Our previous study (6) showed that immunoreactions of VT2c were preferentially localized on the myelin sheaths of nerve fibers in the brain cortexes of mytomycin-treated mice inoculated orally with VT2c-producing *E. coli*. In the present study, we could detect immunoreactions of VT2 on the apical plasma membranes of endothelial cells of hypothalamic capillaries at 24 h after injection of VT2. Death was attributed to the damage in the medulla of the cerebral hemisphere (including an area of white matter), with a brain stem lesion detected by T2-weighted MRI. Furthermore, the immunoactivity of VT2, determined by use of a monoclonal anti-VT2 antibody, was localized in the myelin sheaths of neuron fibers in the brain stem lesion. Taking these facts into consideration, we consider at present that VT2 and VT2c are toxic to nerve fibers and that acute encephalopathy induced by the VTs is a cause of death. Further investigation of Gb_3 (the receptor of VT2) in the rabbit brains is necessary, and such immunohistochemical studies with an anti-Gb_3 monoclonal antibody are now in progress in our laboratory.

Morphological alterations of the nerve fibers induced by VT2 could be compared with those induced by neurotoxic agents. It is well known that a primary neurological lesion is induced by the neurotoxic agents tryiethyltin and hexachlorophene (8, 30, 34). These agents cause intramyelinic nerve edema in the CNS. Despite the extensive involvement of myelin, the ultrastructure of the axoplasm and neural cell bodies appeared to be relatively normal after treatment with these neurotoxic agents. In our electron microscopic findings, intramyelinic edema was found in the lesions of the brain stem and medulla of the cerebral hemisphere. The characteristic destruction of the CNS induced by VT2 has been suggested to impair myelin sheaths and result in demyelination. We thought that these nerve degenerations of the brain stem might be strongly related to a fatal factor. By light microscopy, we reconfirmed the degeneration of the nerve fibers, indicated by swelling and waving.

The bilateral or unilateral hippocampus appeared to be hyperintense and to be accompanied by brain stem lesions. Any neurotoxin that alters the hippocampal function is likely to impair recent memory. Orme et al. (23) reported that HUS patients demonstrated a significantly lower IQ. Temporal lobe epilepsy is frequently accompanied by lesions of the hippocampus (2). Akashi et al. (1) reported that epilepsy is seen in patients who developed HUS associated with VTEC in Japan.

Even though some rabbits escaped damage to the medulla of the cerebral hemisphere or brain stem, these rabbits showed cerebellar lesions at a later date. At 80 h after the injection of VT2, the vermis or the cerebellar hemisphere appeared to be hyperintense. These animals developed an ataxic gait, paralysis in the extremities, and an opisthotonic posture. Riet-Correa et al. (26) reported that a bovine showed cerebellar disorders, which were characterized as seizures, nystagmus, and opisthotonus, after ingestion of *Solanum fastigiatum* var. *fastigiatum*. They suggested that opisthotonus was caused by cerebellar, but not midbrain or pons, damage. Our observations were similar to theirs; that is, our rabbits with cerebellar damage also suffered from opisthotonus. Rabbits in which only the cerebellum was impaired, however, survived with dysfunction for a month. In our study, the high signal intensity in the cerebellar hemisphere was recognized at 1 month after VT2 injection.

Our findings indicated that rabbits challenged with VT2 showed a variety of brain damage, and changes were observed by T2-weighted MRI with the passage of time. The lesions of the medulla in the cerebral hemisphere and the brain stem were associated with mortality of the rabbits. Therefore, MRI techniques may be a useful tool for diagnosing various stages of VTEC infection and its prognosis. Edematous changes in the rabbit brain determined by ultrastructural studies and MRI were due to the toxicity of VT2 which was conveyed from the endothelial and ependymal cell layers.

ACKNOWLEDGMENTS

We thank Sunao Fujimoto and Shin-ichi Kubo for insightful suggestions.

This study was supported by Grant-in-Aid for Scientific Research 08300012 from the Ministry of Education, Science, Sports and Culture, Japan.

REFERENCES

1. **Akashi, S., K. Joh, A. Tsuji, H. Ito, H. Hoshi, T. Hayakawa, J. Ihara, T. Abe, M. Hatori, T. Mori, and T. Nakamura.** 1994. A severe outbreak of haemorrhagic colitis and haemolytic uraemic syndrome associated with *Escherichia coli* O157:H7 in Japan. Eur. J. Pediatr. **153:**650–655.
2. **Babb, T. L., and W. J. Brown.** 1987. Pathological finding in epilepsy, p. 511–540. *In* J. Engl (ed.), Surgical treatment of the epilepsies. Raven Press, New York.
3. **Barrett, T. J., M. E. Potter, and I. K. Wachsmuth.** 1989. Continuous peritoneal infusion of Shiga-like toxin II (SLT II) as a model for SLT II-induced disease. J. Infect. Dis. **159:**774–777.
4. **Bridgwater, F. A. J., R. S. Morgan, K. E. K. Rowson, and G. P. Wright.** 1955. The neurotoxin of *Shigella shigae*. Morphological and functional lesions produced in the central nervous system of rabbits. Br. J. Exp. Pathol. **36:** 447–453.
5. **Francis, D. H., R. A. Moxley, and C. Y. Andraos.** 1989. Edema disease-like brain lesions in gnotobiotic piglets infected with *Escherichia coli* serotype O157:H7. Infect. Immun. **57:**1339–1342.
6. **Fujii, J., T. Kita, S. Yoshida, T. Takeda, H. Kobayashi, N. Tanaka, K. Ohsato, and Y. Mizuguchi.** 1994. Direct evidence of neuron impairment by oral infection with verotoxin-producing *Escherichia coli* O157:H− in mitomycin-treated mice. Infect. Immun. **62:**3447–3453.
7. **Hamano, S., Y. Nakanishi, T. Nara, T. Seki, T. Ohtani, T. Oishi, K. Joh, T. Oikawa, Y. Muramatsu, Y. Ogawa, and S. Akashi.** 1993. Neurological manifestations of hemorrhagic colitis in the outbreak of *Escherichia coli* O157:H7 infection in Japan. Acta Paediatr. **82:**454–458.
8. **Hammond, E. J., and B. J. Wilder.** 1985. Gamma-vinyl GABA. Gen. Pharm. **16:**441–447.
9. **Hii, J. H., C. Gyles, T. Morooka, M. A. Karmali, R. Clarke, S. DeGrandis, and J. L. Brunton.** 1991. Development of verotoxin 2- and verotoxin 2 variant (VT2v)-specific oligonucleotide probes on the basis of the nucleotide sequence of the B cistron of VT2v from *Escherichia coli* E32511 and B2F1. J. Clin. Microbiol. **29:**2704–2709.
10. **Howard, J. G.** 1955. Observations on the intoxication produced in mice and rabbits by the neurotoxin of *Shigella shigae*. Br. J. Exp. Pathol. **36:**439–446.
11. **Jackson, M. P., R. J. Neill, A. D. O'Brien, R. K. Holmes, and J. W. Newland.** 1987. Neucleotide sequence analysis and comparison of the structural genes for Shiga-like toxin I and Shiga-like toxin II encoded by bacteriophages from *Escherichia coli* 933. FEMS Microbiol. Lett. **44:**109–114.
12. **Karmali, M. A.** 1989. Infection by verocytotoxin-producing *Escherichia coli*. Clin. Microbiol. Rev. **2:**15–38.
13. **Karmali, M. A., M. Petric, C. Lim, P. C. Fleming, G. S. Arbus, and H. Lior.** 1985. The association between idiopathic hemolytic uremic syndrome and infection by verotoxin-producing *Escherichia coli*. J. Infect. Dis. **151:**775–782.
14. **Karmali, M. A., B. T. Steele, M. Petric, and C. Lim.** 1983. Sporadic cases of haemolytic-uraemic syndrome associated with faecal cytotoxin and cytotoxin-producing *Escherichia coli* in stools. Lancet **i:**619–620.
15. **Karnovsky, M. J.** 1967. The ultrastructural basis of capillary permeability studied with peroxidase as a tracer. J. Cell. Biol. **35:**213–236.
16. **Kobayashi, N.** 1986 Ekiri, an acute encephalopathy associated with dysentery in Japanese children: a review in retrospect. Acta Paediatr. Jpn. **28:**651–655.
17. **Linggood, M. A., and J. M. Thompson.** 1987. Verotoxin production among porcine strains of *Escherichia coli* and its association with oedema disease. J. Med. Microbiol. **25:**359–362.
18. **Lingwood, C. A., H. Law, S. Richardson, M. Petric, J. L. Brunton, S. DeGrandis, and M. A. Karmali.** 1987. Glycolipid binding of purified and recombinant *Escherichia coli* produced verotoxin in vitro. J. Biol. Chem. **262:** 8834–8839.
19. **Liu, L., T. Kita, N. Tanaka, and Y. Kinoshita.** 1996. The expression of tumor necrosis factor in the hypothalamus after treatment with lipopolysaccharide. Int. J. Exp. Pathol. **77:**37–44.
20. **Lukes, S. A., L. E. Crooks, M. J. Aminoff, L. Kaufman, H. S. Panitch, C. Mills, and D. Norman.** 1983. Nuclear magnetic resonance imaging in multiple sclerosis. Ann. Neurol. **13:**592–601.
21. **Milford, D. V., C. M. Taylor, B. Guttridge, S. M. Hall, B. Rowe, and H. Kleanthous.** 1990. Haemolytic uraemic syndromes in the British Isles 1985–8: association with verocytotoxin producing *Escherichia coli*. 1. Clinical and epidemiological aspects. Arch. Dis. Child. **65:**716–721.
22. **Morrison, D. M., D. L. J. Tyrrell, and L. D. Jewell.** 1986. Colonic biopsy in verotoxin-induced hemorrhagic colitis and thrombotic thrombocytopenic purpura (TTP). Am. J. Clin. Pathol. **86:**108–112.
23. **Orme, S. F., E. Clark, and R. L. Siegler.** 1994. Neuropsychological sequelae of the hemolytic uremic syndrome, abstr. P4.21, p. 88. *In* Abstracts of the 2nd International Symposium and Workshop on Verocytotoxin (Shiga-Like Toxin)-Producing *Escherichia coli* Infections, Bergamo, Italy.
24. **Ostroff, S. M., P. I. Tarr, M. A. Neill, J. H. Lewis, N. Hargrett-Bean, and J. M. Kobayashi.** 1989. Toxin genotypes and plasmid profiles as determinants of systemic sequelae in *Escherichia coli* O157:H7 infections. J. Infect. Dis. **160:**994–998.
25. **Richardson, S. E., T. A. Rotman, V. Jay, C. R. Smith, L. E. Becker, M. Petric., N. F. Olivieri, and M. A. Karmali.** 1992. Experimental verocytotoxemia in rabbits. Infect. Immun. **60:**4154–4167.
26. **Riet-Correa, F., M. D. C. Mendez, A. L. Schild, B. A. Summers, and J. A. Oliveira.** 1983. Intoxication by *Solanum fastigiatum var. fastigiatum* as a cause of cerebellar degeneration in cattle. Cornell Vet. **73:**240–256.
27. **Riley, L. W., R. S. Remis, S. D. Helgerson, H. B. McGee, J. G. Wells, B. R. Davis, R. J. Hebert, E. S. Olcott, L. M. Johnson, N. T. Hargrett, P. A. Blake, and M. L. Cohen.** 1983. Hemorrhagic colitis associated with a rare *Escherichia coli* serotype. N. Engl. J. Med. **308:**681–685.
28. **Rooney, J. C., R. M. Anderson, and I. J. Hopkins.** 1971. Clinical and pathological aspects of central nervous system involvement in the haemolytic uraemic syndrome. Aust. Paediatr. J. **7:**28–33.
29. **Shi, Z.-R., S. H. Itzkowitz, and Y. S. Kim.** 1988. A comparison of three immunoperoxidase techniques for antigen detection in colorectal carcinoma tissues. J. Histochem. Cytochem. **36:**317–322.
30. **Spencer, P. S., G. V. Foster, A. B. Sterman, and D. Horoupian.** 1980. Acetyl ethyl tetramethyl tetralin, p. 296–308. *In* P. S. Spencer and H. H. Schaumburg (ed.), Experimental and clinical neurotoxicology. The Williams & Wilkins Co., Baltimore.
31. **Strockbine, N. A., M. P. Jackson, L. M. Sung, R. K. Holmes, and A. D. O'Brien.** 1988. Cloning and sequencing of genes for Shiga toxin from *Shigella dysenteriae* type 1. J. Bacteriol. **170:**1116–1122.
32. **Takao, T., T. Tanabe, Y.-M. Hong, Y. Shimonishi, H. Kurazono, T. Yutsudo, C. Sasakawa, M. Yoshikawa, and Y. Takeda.** 1988. Identity of molecular structure of Shiga-like toxin 1 (VT1) from *Escherichia coli* O157: H7 with that of Shiga toxin. Microb. Pathog. **5:**357–369.
33. **Tesh, V. L., J. E. Samuel, L. P. Perera, J. B. Sharefkin, and A. D. O'Brien.** 1991. Evaluation of the role of Shiga and Shiga-like toxins in mediating direct damage to human vascular endothelial cells. J. Infect. Dis. **164:**344–352.
34. **Towfighi, J.** 1980. Hexachlorophene, p. 440–455. *In* P. S. Spencer and H. H. Schaumburg (ed.), Experimental and clinical neurotoxicology. The Williams & Wilkins Co., Baltimore.
35. **Tyler, S. D., W. M. Johnson, H. Lior, G. Wang, and K. R. Rozee.** 1991. Identification of verotoxin type 2 variant B subunit genes in *Escherichia coli* by the polymerase chain reaction and restriction fragment length polymorphism analysis. J. Clin. Microbiol. **29:**1339–1343.
36. **Tzipori, S., C. W. Chow, and H. R. Powell.** 1988. Cerebral infection with *Escherichia coli* O157:H7 in humans and gnotobiotic piglets. J. Clin. Pathol. **41:**1099–1103.
37. **Upadhyaya, K., K. Barwick, M. Fishaut, M. Kashgarian, and N. J. Siegel.** 1980. The importance of nonrenal involvement in hemolytic-uremic syndrome. Pediatrics **65:**115–120.
38. **Waddell, T., S. Head, M. Petric, A. Cohen, and C. Lingwood.** 1988. Globotriosyl ceramide is specifically recognized by the *Escherichia coli* verotoxin 2. Biochem. Biophys. Res. Commun. **152:**674–679.
39. **Weinstein, D. L., M. P. Jackson, J. E. Samuel, R. K. Holmes, and A. D. O'Brien.** 1988. Cloning and sequencing of a Shiga-like toxin type II variant from an *Escherichia coli* strain responsible for edema disease of swine. J. Bacteriol. **170:**4223–4230.
40. **Yutsudo, T., N. Nakabayashi, T. Hirayama, and Y. Takeda.** 1987. Purification and some properties of a vero toxin from *Escherichia coli* O157:H7 that is immunologically unrelated to Shiga toxin. Microb. Pathog. **3:**21–30.
41. **Zoja, C., D. Corna, C. Farina, G. Sacchi, C. Lingwood, M. P. Doyle, V. V. Padhye, M. Abbate, and G. Remuzzi.** 1992. Verotoxin glycolipid receptors determine the localization of microangiopathic process in rabbits given verotoxin-1. J. Lab. Clin. Med. **120:**229–238.

Editor: A. O'Brien